

## Measurement and Analysis of Near-Classical Thermal Transport in One-Micron Laser-Irradiated Spherical Plasmas

A. Hauer, W. C. Mead, and O. Willi

*Los Alamos National Laboratory, Los Alamos, New Mexico 87545*

and

J. D. Kilkenny, D. K. Bradley, and S. D. Tabatabaei

*Imperial College, London, United Kingdom*

and

C. Hooker

*Rutherford Appleton Laboratory, Chilton, Didcot, United Kingdom*

(Received 10 August 1984)

Solid spherical layered targets have been uniformly illuminated at irradiances of  $10^{14}$  to  $10^{15}$  W/cm<sup>2</sup>. Extensive diagnostics including time-resolved x-ray emission and optical probing were used to determine the plasma ablation rate and the plasma blowoff conditions. Comparisons with hydrodynamic simulations show that the thermal conduction is well characterized by a flux limit  $f_e = 0.08 \pm 0.02$ , with a steep temperature gradient. The steepness of the heat front was confirmed with time-resolved spectroscopy.

PACS numbers: 52.25.Fi, 52.50.Jm

Knowledge of energy transport from the region of the laser-light absorption to denser portions of laser-produced plasmas is crucial to an understanding of the laser-induced ablation process.<sup>1-3</sup> Extensive recent computer simulation work<sup>3</sup> has led to the expectation that "classical" transport in spherical laser-heated plasmas can generally be approximated by flux-limited diffusion with a flux limiter in the range of  $f_e = 0.06-0.2$ . Early work, largely involving flat targets, indicated strong to moderate inhibition of the heat flux relative to classical predictions.<sup>4</sup> Some of the more recent work involving spherical targets has indicated transport levels closer to classical,<sup>5</sup> with evidence of a penetrating foot in one case.<sup>6</sup> Other work indicates some flux inhibition even in spherical geometry.<sup>7</sup>

In the present experiment we have used a comprehensive set of diagnostics to characterize the plasma conditions and thermal transport in a spherically symmetric plasma. We have made time-resolved spectroscopic measurements (using both low- and moderate- $Z$  radiating ions) of the penetration of the heat front in spherical plasmas. In addition, we have used optical probing to measure simultaneously the density profile of, and the magnetic field in, the underdense plasma. Comparisons with hydrodynamic modeling show that (a) all observables are consistent with a high flux limit and (b) the heat front shows no observable foot.

The targets used in this study consisted of solid glass spheres ( $\sim 160$   $\mu\text{m}$  diameter), containing Si and Ca (among other constituents), coated with

three layers: (1) CH (0.5 to 2.5  $\mu\text{m}$  thick), (2) Al (0.1  $\mu\text{m}$ ), and (3) CH (0.5 to 2.5  $\mu\text{m}$ ). The solid glass ball prevented implosion of the target (and subsequent inward movement of the critical surface).

The targets were uniformly illuminated with the six-beam, 1.06- $\mu\text{m}$ , laser facility at the Rutherford Appleton Laboratory.<sup>8</sup> The six beams were focused by  $f/1$  lenses with optical axes along the faces of a cube. Incident irradiance levels were in the range  $(1.5-15) \times 10^{14}$  W/cm<sup>2</sup>. The laser pulse had an approximately Gaussian temporal profile with 0.83-ns full width at half maximum (FWHM).

The radial intensity profiles of the beams were measured. Small-scale structure results in about 30% rms variation in intensity. The overlap of the six beams and beam-to-beam energy variation resulted in about 50% (peak-to-valley) large-scale variation in incident irradiance across the surface of the sphere.<sup>9</sup>

The primary diagnostic of thermal transport was time-resolved x-ray line spectroscopy. X-ray line emission was observed first from the thin aluminum layer (sensing temperatures of 200-350 eV) and later from the silicon ( $\sim 250-400$  eV) and calcium ( $\sim 500-700$  eV) in the glass ball.<sup>10</sup>

X-ray emission from the target was dispersed (with a thallium acid phthalate crystal) onto the slit of a streak camera covering 1.7 to 2.4 eV. The spectral and temporal resolutions were about 500 ( $\lambda/\Delta\lambda$ ) and 50 ps, respectively. A seventh laser beam with very short duration ( $\sim 100$  ps) was used

to generate an x-ray fiducial which references the x-ray spectra to the temporal profile of the laser. The density profile of the underdense plasma ( $n_e < n_c$ ) was measured with a 40-ps, 0.35- $\mu\text{m}$  interferometric probe and the magnetic field was measured with a 20-ps, 0.62- $\mu\text{m}$  Faraday rotation probe (probing densities up to  $0.6n_c$ ).

We adjusted laser focusing to achieve good illumination uniformity while minimizing refraction. Spherical symmetry of the plasma was diagnosed with a Faraday rotation probe (sensing large-scale magnetic fields due to nonuniformity), multi-energy-band x-ray pinhole imaging (as an indicator of plasma heating), and the interferometric probe (indicating uniformity of blowoff). It was found that, for tangential illumination, symmetric uniform x-ray photographs (to within 10%) were obtained with negligible (large scale) magnetic field generation ( $< 100$  kG in the underdense plasma). Examples of three diagnostics demonstrating the degree of plasma uniformity are given in Fig. 1. Thermal smoothing<sup>11</sup> of laser irradiance nonuniformities plays an important role in determining the good symmetry seen in Fig. 1.

For uniform illumination, the absorbed fraction measured in these experiments (with ion calorimetry) ranged from 32% to 23% over the incident irradiance range of  $(1.5 \text{ to } 15) \times 10^{14} \text{ W/cm}^2$ .

For incident irradiance of about  $5 \times 10^{14} \text{ W/cm}^2$ , the hot-electron temperature, as measured from the x-ray continuum slope (with a seven-channel diode array) was about 3–6 keV. Inner-shell ( $K\alpha$ ) radiation was observed from solid vanadium targets (of the same diameter as the multilayer targets) coated with various layers of plastic. Faraday-cup ion detection showed immeasurably small energy in fast ions. All of these observations are consistent with less than 3% of incident laser energy present in hot electrons.

Throughout this work, we have used LASNEX<sup>12</sup> Lagrangian hydrodynamic simulations to predict and analyze the experimental results. The modeling included non-local-thermodynamic-equilibrium atomic physics, multigroup flux-limited radiation diffusion, and multigroup flux-limited diffusion for the suprathermal (and all laser-heated) electrons, consistent with earlier work.<sup>13</sup> Electron thermal transport is modeled by single-group flux-limited diffusion. We used resonance-absorption deposition fractions of 0–10% to explore the sensitivity of the results to hot electrons. Inverse bremsstrahlung was cut off above  $0.6n_c$  to account roughly for refraction. With this correction, the calculated absorption agreed well with that measured. The mass ablation rate for a given absorbed intensity was not significantly affected by this correction.

An example of a portion of a time-resolved x-ray line spectrum and a corresponding LASNEX calculation (modeling this specific shot) is given in Fig. 2. A flux limit of 0.1 was used in this calculation. We are primarily concerned here with the initial penetration of the heat front. The calculations were made for a thin layer near the surfaces of the aluminum and silicon. This predicts the rise of the radiation accurately, but not the full time history. Both theory and experiment show a very rapid rise ( $< 100$  ps) for the onset of aluminum and silicon emission.

Mass ablation rates can be obtained from the time-resolved spectra by taking the delay between aluminum and silicon emission as the time needed to ablate the plastic layer between them. In Fig. 3, we plot the specific mass ablation rate versus absorbed irradiance (referenced to the initial surface area). The experimental points on this graph were chosen so that the burnthrough interval occurred within  $\pm 400$  ps of the peak of the pulse.

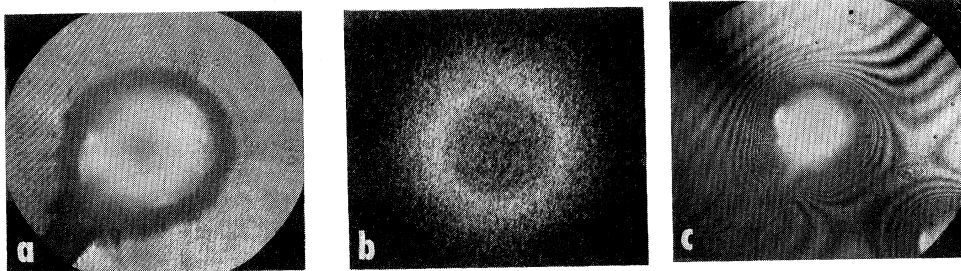


FIG. 1. Three diagnostics of plasma symmetry characteristics. (a) Faraday rotation probe implies  $B < 100$  kG, (b) x-ray pinhole photograph ( $\sim 1$  keV) indicates uniform heating, (c) interferogram indicates blowoff uniformity to  $\sim 10$ –15%.

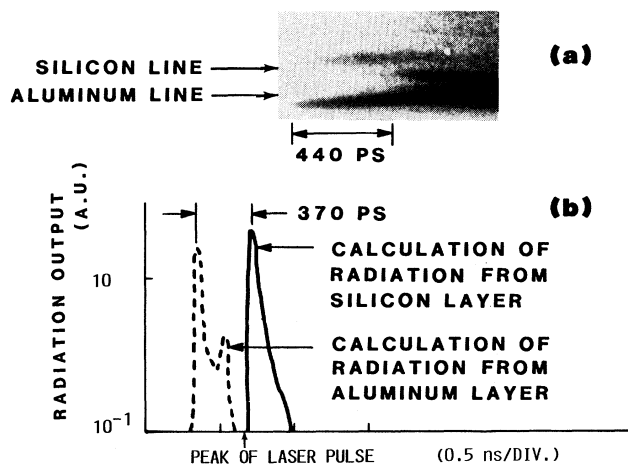


FIG. 2. Comparison between LASNEX hydrodynamic simulation and experiment. (a) Spectrally resolved x-ray streak; (b) calculated ( $f_e = 0.1$ ) emission from Al and Si layers. (The aluminum line identified is  $1s^2-1s3p$  and the silicon line is a satellite to  $1s^2-1s2p$ .) The calculated emission shown is that of the outer zone of the Al and glass layers, and so it decreases more rapidly than that measured.

We also show, in Fig. 3, the results of the simulations for various flux limiters. The bands shown reflect the calculated sensitivity of  $\dot{m}$  to time-dependent and refractive effects. As shown in the figures, the transport is inhibited over the entire intensity range of this experiment, for values of  $f_e < 0.1$ . The transport and plasma conditions are insensitive to the flux limit for  $f_e > 0.1$ . That is, the transport in this regime is conduction limited. Good agreement is obtained for  $f_e \approx 0.08 \pm 0.02$ . To determine an upper limit on the effects of hot electrons, some calculations were performed under the assumption that 10% of the energy reaching the critical surface was absorbed into a distribution with  $T_{hot} = 5$  keV. The added hot electrons increases the heat front penetration by about 20%, on the assumption of equal thermal and suprathermal flux limits. This would not significantly alter the inferred flux limit.

Also shown in Fig. 3 is a summary of data in two recent studies of mass ablation performed by Tarvin *et al.*<sup>7</sup> and points taken by Yaakobi *et al.*<sup>6</sup> The data of Ref. 7 agree reasonably well with the present work while those of Ref. 6 are somewhat higher. Our calculations (and the measured density profiles) suggest that temperature gradients are steeper in the work of Tarvin *et al.* because of differences in experimental parameters. This is consistent with their inference of a lower flux limit ( $f_e = 0.03-0.06$ ) from similar mass ablation data. We

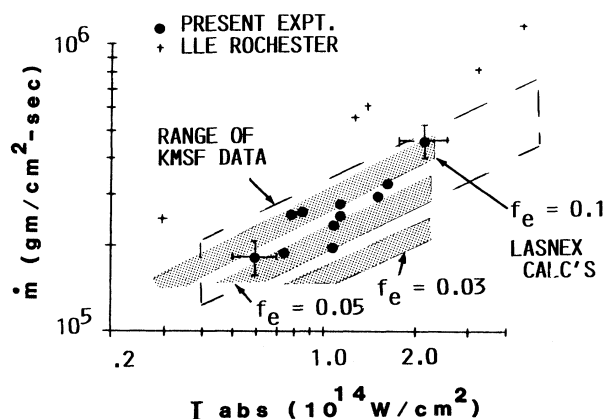


FIG. 3. Mass ablation rates as a function of absorbed irradiance.

cannot presently account for the differences between our  $\dot{m}$  measurements and those of Yaakobi *et al.*

Time-resolved measurements of calcium emission from the glass were also made. In Fig. 4, we show streak traces of a calcium and a silicon line. For the usual tangentially focused shots, a very small delay ( $< 100$  ps) was observed between the

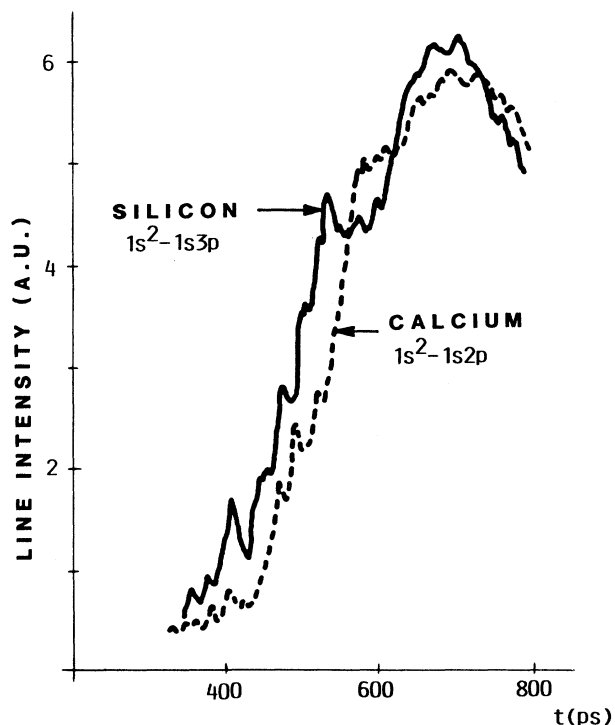


FIG. 4. Temporal profile of x-ray lines coming from the glass. Nearly simultaneous onset of Si and Ca indicates a steep heat front.

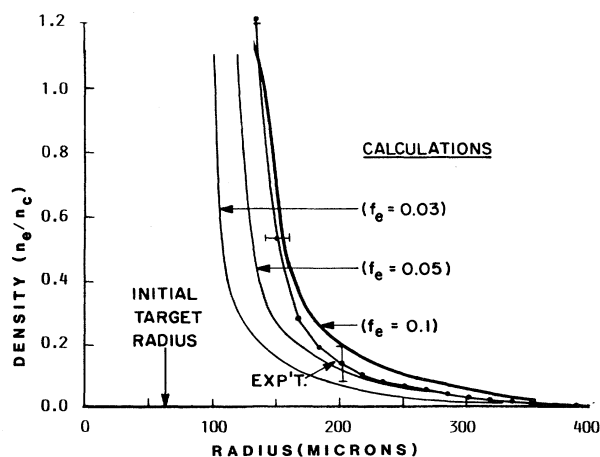


FIG. 5. Experimental density profile taken at the peak of the laser pulse compared with modeling. Incident intensity  $\sim 8 \times 10^{14}$  W/cm<sup>2</sup>.

turnon of silicon and calcium line emission. The rise time between the effective radiating temperatures of silicon and calcium is thus a small fraction of the burnthrough interval. This indicates a relatively steep heat front, and is consistent with the LASNEX non-local-thermodynamic-equilibrium calculations.

As an additional test of the modeling, we compared the measured and calculated plasma density profiles. The steepness and outward motion of the density contours are indicators of the ablated mass fraction and are thus sensitive to electron energy transport. In Fig. 5, we show an example of such a comparison. A flux limit  $f_e \approx 0.05$ – $0.1$  gives the best agreement.

In conclusion, we find that the thermal-electron transport in these spherical target experiments is best described by near-classical modeling ( $f_e = 0.08 \pm 0.02$ ). Our calculations have shown that a given measured  $\dot{m}$  can lead to somewhat different inferred flux limits, depending on experimental parameters such as the temperature gradient. Good plasma symmetry characteristics were established and carefully diagnosed. The effects of coronal magnetic fields were minimized. The observation of little time delay between emission from silicon

and calcium indicates a relative steep heat front and is consistent with the modeling.

We gratefully acknowledge the contributions of the Rutherford Appleton Laboratory Laser Division staff. We would like to thank O. Landen for valuable experimental assistance. We also thank the Los Alamos target fabrication group for their excellent work on the targets used in this study. Dwight Duston and Jack Davis of the U. S. Naval Research Laboratory provided valuable advice on spectral analysis. We would like to thank Phil Goldstone for valuable advice in planning and analyzing this experiment. Portions of this work were sponsored by the U. S. Department of Energy and by the Science and Engineering Research Council (U.K.).

<sup>1</sup>R. C. Malone, R. L. McCrory, and R.L. Morse, Phys. Rev. Lett. **14**, 721 (1975); R. A. Haas *et al.*, Phys. Fluids **20**, 322 (1977).

<sup>2</sup>C. E. Max, C. F. McKee, and W. C. Mead, Phys. Fluids **23**, 1620 (1980), and references therein.

<sup>3</sup>R. J. Bickerton, Nucl. Fusion **13**, 457 (1973); R. J. Mason, Phys. Rev. Lett. **47**, 652 (1981); A. R. Bell, R. G. Evans, D. J. Nicholas, Phys. Rev. Lett. **46**, 243 (1981); J. P. Matte and J. Virmont, Phys. Rev. Lett. **49**, 1936 (1982).

<sup>4</sup>F. C. Young *et al.*, Appl. Phys. Lett. **30**, 45 (1977); B. Yaakobi and T. Bristow, Phys. Rev. Lett. **38**, 350 (1977); W. L. Kruer, Comments Plasma Phys. Controlled Fusion **5**, 69 (1979); D. L. Banner and W. C. Mead, Lawrence Livermore National Laboratory Laser Program Annual Report No. UCRL-50021-79, 1980 (unpublished), pp. 6–12.

<sup>5</sup>T. Goldsack *et al.*, Phys. Fluids **25**, 9 (1982).

<sup>6</sup>B. Yaakobi *et al.*, Phys. Fluids **27**, 516 (1984).

<sup>7</sup>J. Tarvin *et al.*, Phys. Rev. Lett. **51**, 1355 (1983).

<sup>8</sup>I. N. Ross *et al.*, IEEE J. Quantum Electron. **17**, 1653 (1981).

<sup>9</sup>I. N. Ross, Opt. Commun. **43**, 350 (1982).

<sup>10</sup>Estimates of effective radiating temperatures are for local thermodynamic equilibrium conditions at a density slightly above critical.

<sup>11</sup>S. Obenschain *et al.*, Phys. Rev. Lett. **46**, 1402 (1981); A. J. Cole, J. Phys. D **15**, 1689 (1982).

<sup>12</sup>G. Zimmerman and W. Kruer, Comments Plasma Phys. Controlled Fusion **2**, 85 (1975).

<sup>13</sup>W. C. Mead *et al.*, Phys. Fluids **5**, 1301 (1984).

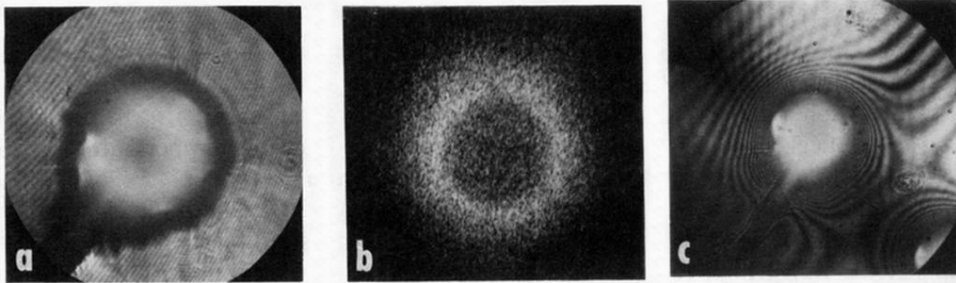


FIG. 1. Three diagnostics of plasma symmetry characteristics. (a) Faraday rotation probe implies  $B < 100$  kG, (b) x-ray pinhole photograph ( $\sim 1$  keV) indicates uniform heating, (c) interferogram indicates blowoff uniformity to  $\sim 10$ – $15\%$ .

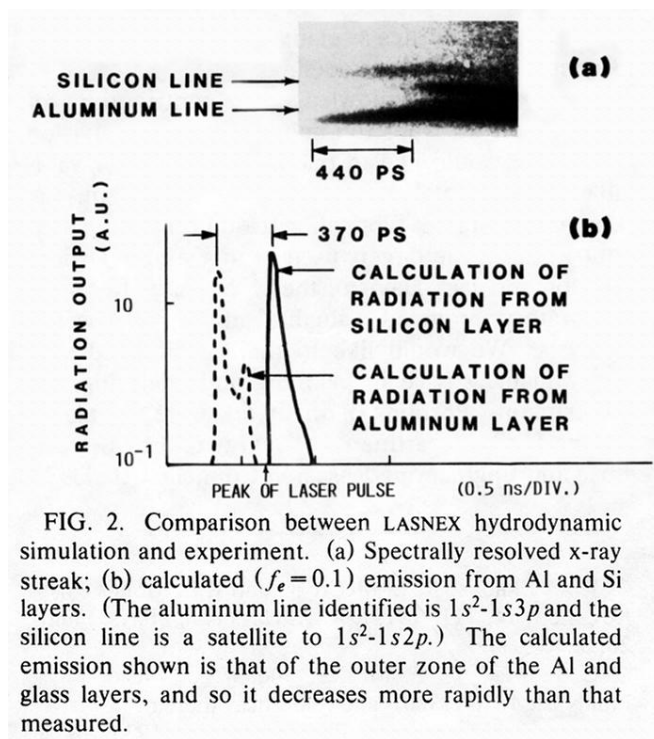


FIG. 2. Comparison between LASNEX hydrodynamic simulation and experiment. (a) Spectrally resolved x-ray streak; (b) calculated ( $f_e = 0.1$ ) emission from Al and Si layers. (The aluminum line identified is  $1s^2-1s3p$  and the silicon line is a satellite to  $1s^2-1s2p$ .) The calculated emission shown is that of the outer zone of the Al and glass layers, and so it decreases more rapidly than that measured.